



Effect of Cerium Oxide Nanoparticles on Myocardial Cell Apoptosis Induced by Myocardial Ischemia-Reperfusion Injury

Yudan Zhao¹, Yahan Yang¹, Yishu Wen¹, Maolin Zhao², Yifei Dong^{3*}

¹Queen Mary College, Nanchang University, Nanchang 330000, Jiangxi, China

²Department of Cardiology, Yingshan People's Hospital, Huanggang, 438700, Hubei, China

³Department of Cardiology, The Second Affiliated Hospital of Nanchang University, Nanchang 330000, Jiangxi, China

ARTICLE INFO

Original paper

Article history:

Received: September 09, 2021

Accepted: March 03, 2022

Published: March 31, 2022

Keywords:

cerium oxide nanoparticles, myocardial ischemia-reperfusion injury, apoptosis index of cardiomyocytes, myocardial cell apoptosis

ABSTRACT

This study was to provide a theoretical basis for effective treatment of myocardial ischemia-reperfusion injury (I/R injury) and explore the effect of cerium oxide (CeO₂) nanoparticles on myocardial cell apoptosis induced by I/R injury. In this study, 50 healthy male Sprague Dawley (SD) rats were selected and divided into five groups according to the random table method: a sham operation group, an I/R group, a 1 - 10 nm CeO₂ nanoparticle group (CeO₂-1 group), a 10 - 25 nm CeO₂ nanoparticle group (CeO₂-2 group), and a 50 nm CeO₂ nanoparticle group (CeO₂-3 group). Rats in different groups were injected with phosphate buffer solution (PBS) and CeO₂ nanoparticles with different diameters, respectively. The rat models of I/R injury were prepared to explore and analyze the superoxide dismutase (SOD) activity, malondialdehyde (MDA) content, glutathione peroxidase (GSH-Px) activity, and myocardial cell apoptosis of rats with I/R injury by CeO₂ nanoparticles. The results showed that the cardiomyocyte necrosis, SOD activity, MDA content, GSH-Px activity, and apoptosis index of the three groups of rats injected with CeO₂ nanoparticles were much better than those in the I/R group. The effects on SOD activity, MDA content, GSH-Px activity, and apoptosis index of cardiomyocytes in the CeO₂-2 group were significantly better than those in the CeO₂-1 and CeO₂-3 groups, showing statistically great differences ($P < 0.05$); and effects on SOD activity, MDA content, and GSH-Px activity of cardiomyocytes in CeO₂-1 group were better obviously than those in the CeO₂-3 groups, showing statistically observable differences ($P < 0.05$). In addition, the difference between the CeO₂-1 group and CeO₂-3 on the apoptosis index of cardiomyocytes was not statistically remarkable ($P > 0.05$). It can be considered that the CeO₂ nanoparticles can effectively alleviate the effects of myocardial I/R injury, showing reliable clinical significance.

DOI: <http://dx.doi.org/10.14715/cmb/2022.68.3.6>

Copyright: © 2022 by the C.M.B. Association. All rights reserved.



Introduction

The number of deaths caused by cardiovascular diseases (CVDs) accounts for a large part of the total deaths in the world, and CVDs will be regarded as the most important cause of human life safety with the improvement of people's living standards (1,2). A large number of ischemic heart diseases cause insufficiency of blood supply to the heart in patients, leading to adverse events such as myocardial infarction and sudden death (3). Fast and effective restoration of blood supply in patients has become the key to the treatment of ischemic heart disease. Clinically, cardiac stents and drug treatments are mainly used to improve the recanalization rate of blood vessels, thereby improving ischemic heart disease (4). The restoration of blood supply is very important to resist myocardial cell apoptosis, but the

local oxidative stress response of cardiomyocytes will also be generated when the blood supply is restored, resulting in cardiomyocyte damage, which is myocardial ischemia-reperfusion injury (I/R injury) (5). After the blood supply is restored, patients often experience adverse events such as cardiac insufficiency and arrhythmia, which cause the patient's life status to be worse than the condition during ischemia (6). Preventing or mitigating myocardial cell I/R injury has attracted the attention of many scholars (7). Studies have shown that oxygen free radicals, pH, and calcium ions affect I/R injury (8). With the further development of science and technology, there are more and more methods to treat myocardial cell I/R injury, but there are few clear methods that can be effectively treated, and myocardial ischemic preconditioning (IPC) is one of

*Corresponding author. E-mail: longsirong50211225@163.com
Cellular and Molecular Biology, 2022, 68(3): 43-50

them (9). Myocardial IPC refers to the short-term use of various methods to make the myocardium undergo one or more ischemic processes before prolonged ischemia, so as to have a certain tolerance to the subsequent ischemic process, thereby reducing the damage of I/R injury to cardiomyocytes (10).

As a cheap rare earth oxide, cerium oxide (CeO_2) has gradually entered people's sight because of the large number of ion vacancies on its surface, which makes Ce^{3+} ions on the surface of the particles (11). CeO_2 nanoparticles can change with the environment. The ions on its surface can change back and forth between Ce^{3+} and Ce^{4+} , which can effectively play an anti-oxidation effect. They have been widely used in many research fields, such as high-temperature oxidation protection materials and solar energy battery power generation (12). Studies have also found that CeO_2 nanoparticles have the effect of antioxidant enzymes, which can protect against a variety of tissue damage and organ damage caused by oxygen free radicals by scavenging the biological properties of oxygen free radicals (13). Experiments have shown that 30 days after the injection of CeO_2 nanoparticles into experimental animals, the animals did not undergo significant tissue changes, and they were well tolerated and did not increase mortality (14). CeO_2 nanoparticles are rich in resources in China, and the preparation process is relatively simple. Therefore, exploring the potential of CeO_2 nanoparticles and developing their advantages of non-toxic side effects is of important clinical significance (15).

In this study, a rat model of myocardial I/R injury was prepared and injected with CeO_2 nanoparticles of different diameters to measure and compare the superoxide dismutase (SOD) activity, malondialdehyde (MDA) content, glutathione peroxidase (GSH-Px) activity; in addition, the myocardial cell apoptosis was measured, aiming to provide a theoretical basis for the application of CeO_2 nanoparticles in the clinical treatment of ischemic CVDs.

Materials and methods

Research subjects and grouping

CeO_2 nanoparticles and phosphate-buffered saline (PBS) solution were purchased and other reagents were commercially available. 50 healthy and specified pathogen-free (SPF) male Sprague Dawley (SD) rats,

weighing 250 - 300 g in total, were purchased and raised at the experimental center of Yingshan People's Hospital. The experiment process followed the "ethical principles of animal testing". The rats were randomly divided into 5 groups according to the random table method, with 10 rats in each group. The specific groups were as follows:

Sham group: PBS buffer (2 mL/kg) was injected intravenously 1 day before the surgery; the chest was opened, and the left anterior descending coronary artery was only threaded and not ligated.

Model group: PBS buffer (2 mL/kg) was injected intravenously 1 day before surgery to prepare an I/R model.

CeO_2 -1 group: one day before the operation, CeO_2 nanoparticle suspension (2mL / kg) with a diameter of 1 - 10nm was injected intravenously, and then the I/R model was prepared.

CeO_2 -2 group: one day before the operation, CeO_2 nanoparticle suspension (2mL / kg) with a diameter of 10 - 25nm was injected intravenously, and then the I/R model was prepared.

CeO_2 -3 group: one day before the operation, CeO_2 nanoparticle suspension (2mL / kg) with a diameter of 50nm was injected intravenously, and then the I/R model was prepared.

Preparation of I/R injury model

Firstly, the healthy male SD rats were adaptively reared for one week, fasted for 12 hours before model preparation, and then the myocardial I/R injury rat model was prepared. The healthy male rats with a weight range of 250 g~ 300 g were selected, and anesthetized by intraperitoneal injection. The drug was chloral hydrate with a dose of 300 mg/kg. After sufficient anesthesia, the rats were fixed in the supine position and disinfected at the neck and chest skin. The trachea of the rat was fully separated to expose the trachea. The incision was cut between the tracheal rings for tracheal intubation, and the trachea was fully fixed with surgical tape to prevent it from falling off. The rat's skin was cut at the most obvious place of the left edge of the rat's sternum, the chest was entered in the 4th and 5th intercostal space, and the rat myocardial capsule was torn so that the heart was fully exposed to the air. The thread was performed at the pulmonary artery cone and left atrial appendage about 3 to 4 mm away from the aortic root, and a

grooved latex tube was placed on the ligation line and the surface of the heart. After the rat's heart rate was regular, the left anterior descending coronary artery of the rat was ligated. It can determine whether the ligation was successful or not according to the color of the myocardium at the distal end of the ligation line. If the color changed to white and then to cyan, the ligation was successful. About 45 minutes after the ligation was successful, the ligature was released, and the rat heart was reperfused for about 2 hours. If the color of the rat myocardial ischemic site returned to the normal color, it was determined that the myocardial I/R injury rat model was successfully prepared.

Research methods

After the rat model of myocardial I/R injury was verified by an electrocardiogram test, the rat was subjected to cardiac reperfusion. After 2 hours, the experimental rat was quickly sacrificed and the heart was taken out. The neophyte tissue of the rat left ventricle with confirmed hemorrhage was cut, and the residual blood was fully washed using the cold-treated normal saline. One part was fully fixed in 10% formaldehyde solution for detection of cell apoptosis and myocardial histopathological observation, and the other part was dried with filter paper and placed in a cryopreservation tube and then quickly stored at -80°C in a low-temperature refrigerator.

The rat myocardial specimen stored in a low-temperature refrigerator at -80°C was taken out, weighed, and placed in a beaker. The pre-cooled normal saline was transferred to the beaker with a pipette (the normal saline should be 9 times the weight of the myocardial specimen, and the transferred amount of normal saline was $2/3$ of the total). The myocardial specimen tissue was cut quickly, poured into the homogenization tube, and then mixed fully with the remaining normal saline at a uniform speed. The homogenate tube was placed in ice water for grinding operation until the myocardial tissue was completely crushed. After grinding, 10% was taken for full centrifugation to transfer the supernatant to a sterile tube for detection of SOD activity, MDA content, and GSH-Px activity.

Experimental criteria

The SOD activity of myocardial tissue was generated by the reaction system of xanthine and xanthine oxidase to generate oxygen anions, which can react with hydroxylamine groups to form nitrite. After the nitrite reacted with the color reagent, it became purple-red. The optical density (OD) was detected with a spectrophotometer. Myocardial tissue in rats with myocardial I/R injury contained superoxide dismutase, which would reduce the formation of internal nitrite, so that the measured absorbance value would be lower than that of the control tube, thereby detecting the SOD activity of myocardial tissue. The calculation equation was given as follows:

Total SOD activity (mprot/ml) = (OD in control tube - measured OD) \div OD in control tube \div 50% \times total volume of reaction solution sample volume (ml) \div proxy sample protein concentration (mprot/mL)

In which, mprot/ml represented the number of milligrams of protein.

The principle of detection of MDA content was that oxygen free radicals can react with polyunsaturated fatty acids on the cell membrane to produce lipid peroxidation to generate MDA. This reaction can convert reactive oxygen species into reactive chemicals in large tissues. Therefore, the content of MDA can effectively reflect the degree of lipid peroxidation in the tissue, and thus simply reflect the degree of cell damage. The calculation equation was given as follows:

MDA content (nmol/mgprot) = (OD of the measured tube - OD of the measured blank tube) \div (OD in the standard tube - OD in standard blank tube) \times standard concentration (10 nmol/mL) \div proxy sample protein concentration (mgprot/mL)

In the above equation, nmol/mgprot represented the nanomole/mg protein.

Glutathione peroxidase (GSH-Px) was widely distributed in the body and can specifically catalyze the reaction of reduced glutathione and hydrogen peroxide to protect the integrity of cell membranes. The GSH-Px activity can be expressed by the speed of the enzymatic reaction, and it can be obtained by measuring the consumption speed of reduced glutathione. The calculation equation could be expressed as follows:

GSH-Px activity (u/mgprot) = (OD in a non-enzyme tube - OD in enzyme tube) ÷ (OD in a standard tube - OD in a blank tube) × concentration (20 μmol/L) in standard tube × dilution factor ÷ reaction time ÷ (sampling volume × Sample protein content)

Normal or proliferating cells had almost no deoxyribonucleic acid (DNA) breaks. After the cells underwent apoptosis, endogenous nucleases were activated, causing DNA double-strand or single-strand breaks and the appearance of 3'-OH ends. Deoxyribonucleotide terminal transferase can transfer deoxyribonucleotides to the 3'end of DNA to detect cell apoptosis. This method was called deoxyribonucleotide terminal transferase-mediated gap end labeling law. Under the light microscope, the nucleus of normal cardiomyocytes was blue, and the nucleus of apoptotic cardiomyocytes was brown. 3 slices were selected from one rat, and each slice was observed with 10 high-power fields of 400× to observe the number of apoptotic cells. The percentage was undertaken as the apoptosis index to reflect the myocardial cell apoptosis in rats. Making rat myocardial tissue slices required multiple steps such as dewaxing, hydration, cell permeation, color development, and dehydration. The specific process was shown in the following Figure 1:

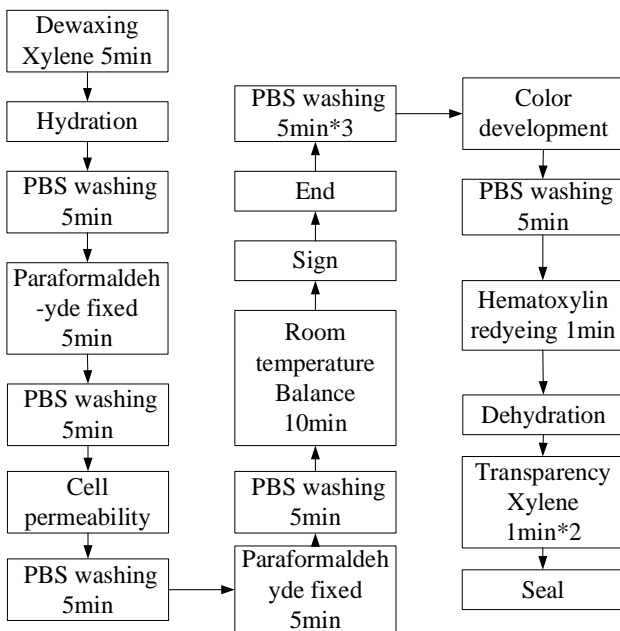


Figure 1. Process of making myocardial tissue slices.

Statistical methods

The SPSS22.0 software was adopted for statistical analysis. The count data were expressed as the number of cases or percentages, and the chi-square test was used for comparison (sensitivity and specificity were compared using paired chi-square test). Measurement data were expressed as mean ± standard deviation, and compared with t-test. The inspection level was defined as α = 0.05. When P was less than 0.05, the difference was considered to be statistically significant.

Results and discussion

Validation of myocardial I/R injury model

One of the model rats was selected randomly and performed with Electrocardiograph (ECG) testing before and after the surgery to verify the success of the preparation of the myocardial I/R injury rat model. Figure 2 was the preoperative ECG result of the rat, and Figure 3 showed the postoperative ECG result of the rat. After comparison, it was found that the rat model of myocardial I/R injury had been successfully prepared.

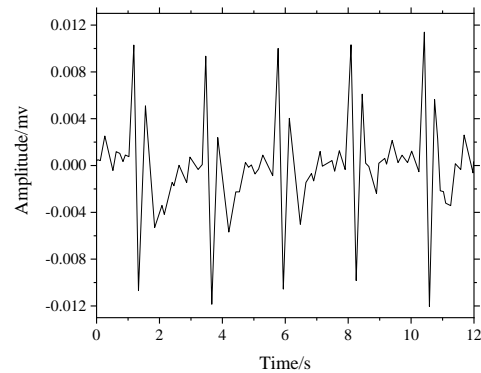


Figure 2. The preoperative ECG result of rats under normal conditions. Note: the heart function of the rate was normal conduction before surgery.

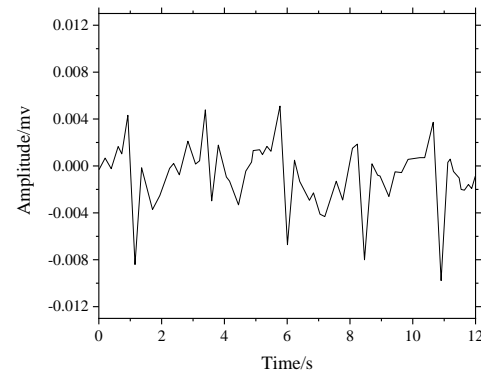


Figure 3. ECG result of a rat from the I/R injury model. Note: compared with the normal ECG result, the ST2 segment of model rats was elevated obviously.

Cardiomyocyte necrosis status of five groups of rats

The morphological structure of the cardiomyocytes of rats was observed under an optical microscope. The results showed that there was no obvious necrosis of cardiomyocytes in the sham group (Figure 4A), there was obvious cardiomyocyte necrosis in the I/R group (Figure 4B), and the three groups of rats injected with CeO₂ nanoparticles had better cardiomyocyte integrity than the I/R group (Figures 4C ~ 4E).

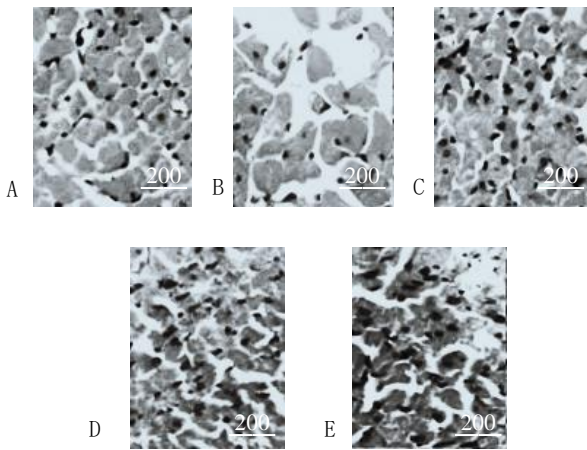


Figure 4. Cardiomyocyte necrosis status of five groups of rats. Note: Figures A and B showed the results in the sham and I/R group, respectively; and Figures C, D, and E showed the results in the CeO₂-1 group, CeO₂-2 group, and CeO₂-3 group, respectively.

Therefore, the cardiomyocytes of the I/R group were obviously swollen, the boundaries were blurred, and there were a large number of inflammatory cells and red blood cell infiltration in the intercellular substance. The three groups of rats injected with CeO₂ nanoparticles showed greatly reduced interstitial edema compared with the I/R group, with little inflammatory cells and red blood cell infiltration.

SOD activity of myocardial tissue in rats with I/R injury

As illustrated in Figure 5, in rat I/R injury myocardial tissue, the SOD activity of the model group was remarkably lower than that of the sham group, and the difference was statistically significant ($P < 0.05$); the SOD activities in three groups injected with different diameters of CeO₂ nanoparticles were much higher in contrast to the model group, showing statistically obvious difference ($P < 0.05$); and the SOD activity in CeO₂-2 group was obviously higher

than that of the two groups, and that in the CeO₂-1 group was observably higher compared with that in the CeO₂-3 group, showing statistically great differences ($P < 0.05$).

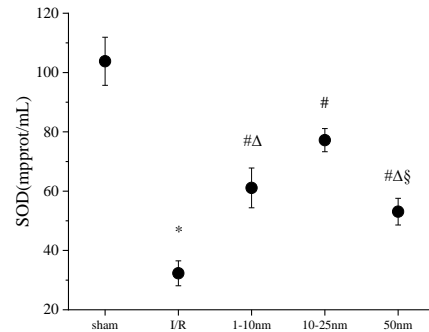


Figure 5. SOD activity of myocardial tissue in rats with I/R injury. Note: *, #, Δ, and § represented the difference was statistically obvious in contrast to the value in sham group, the I/R group, the CeO₂-2 group, and the CeO₂-1 group, respectively ($P < 0.05$).

Changes of MDA content in myocardial tissue of rats with I/R injury

As illustrated in Figure 6, in rat I/R injury myocardial tissue, the MDA content of the I/R model group was remarkably higher than that of the sham group, and the difference was statistically significant ($P < 0.05$); the MDA content in three groups injected with different diameters of CeO₂ nanoparticles were much lower in contrast to the model group, showing statistically obvious difference ($P < 0.05$); and the MDA content in CeO₂-2 group was obviously lower than that of the two groups, and that in the CeO₂-1 group was observably lower compared with that in the CeO₂-3 group, showing statistically great differences ($P < 0.05$).

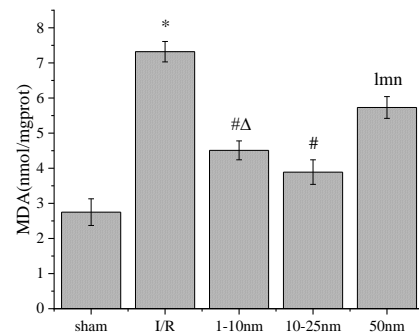


Figure 6. MDA content of myocardial tissue in rats with I/R injury. Note: *, #, Δ, and § represented the difference was statistically obvious in contrast to the value in the sham group, the I/R group, the CeO₂-2 group, and the CeO₂-1 group, respectively ($P < 0.05$).

The GSH-Px activity of myocardial tissue in rats with I/R injury

As illustrated in Figure 7, in rat I/R injury myocardial tissue, the GSH-Px activity of the model group was remarkably lower than that of the sham group, and the difference was statistically significant ($P < 0.05$); the GSH-Px activities in three groups injected with different diameters of CeO₂ nanoparticles were much higher in contrast to the model group, showing statistically obvious difference ($P < 0.05$); and the GSH-Px activity in CeO₂-2 group was higher than that of the two groups, and that in the CeO₂-1 group was observably higher compared with that in the CeO₂-3 group, showing statistically great differences ($P < 0.05$).

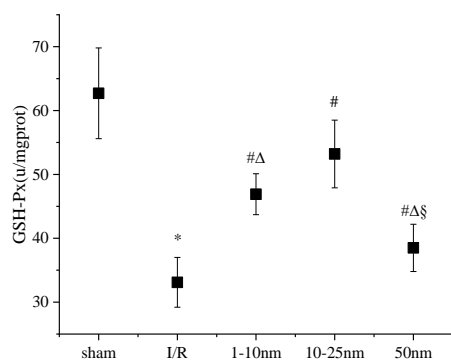


Figure 7. The GSH-Px activity of myocardial tissue in rats with I/R injury. Note: *, #, Δ, and § represented the difference was statistically obvious in contrast to the value in the sham group, the I/R group, the CeO₂-2 group, and the CeO₂-1 group, respectively ($P < 0.05$).

Changes of apoptotic cells in myocardial tissue of rats with I/R injury

As illustrated in Figure 8, in rat I/R injury myocardial tissue, the myocardial cell apoptosis index of the I/R model group was remarkably higher than that of the sham group, and the difference was statistically significant ($P < 0.05$); the myocardial cell apoptosis indexes in three groups injected with different diameters of CeO₂ nanoparticles were much lower in contrast to the model group, showing statistically obvious difference ($P < 0.05$); the myocardial cell apoptosis index in CeO₂-2 group was lower than that of the two groups, showing statistically great differences ($P < 0.05$); and that in the CeO₂-1 group was not observably different compared with that in the CeO₂-3 group ($P > 0.05$).

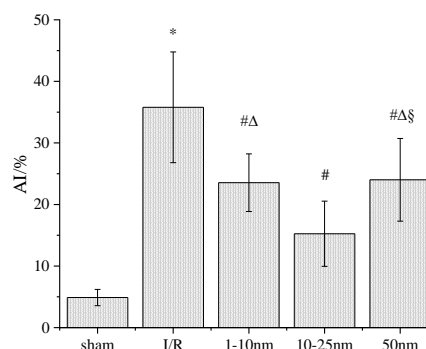


Figure 8. Cell apoptosis index of myocardial tissue in rats with I/R injury. Note: *, #, Δ, and § represented the difference was statistically obvious in contrast to the value in the sham group, the I/R group, the CeO₂-2 group, and the CeO₂-1 group, respectively ($P < 0.05$).

Myocardial I/R injury has had a non-negligible impact on human life and health. Studies have found that in the process of ischemia and reperfusion, the main reason is the explosive production of a large number of oxygen free radicals (16). The oxygen-free radicals generated during I/R injury will react to produce malondialdehyde, which will further affect the cells, so the MDA content can effectively reflect the degree of ischemia-reperfusion injury (17). The human body also has its scavenging mechanism for oxygen-free radicals. Among them, GSH-Px scavenges hydrogen peroxide and lipid peroxides to protect cells, while SOD reduces MDA in the body through disproportionation, and further alleviates cell damage caused by ischemia-reperfusion through GSH-Px (18).

There are various applications for nanomaterials (19-22). After experimental comparison, it was found that compared with the model group, the SOD activity and GSH-Px activity in the myocardial tissue cells of the three groups injected with different diameters of CeO₂ nanoparticles were remarkably increased, and the MDA content in the myocardial cells was also greatly reduced, showing statistically visible differences ($P < 0.05$). The comparison of three groups injected with different diameters of CeO₂ nanoparticles revealed that the effect of the CeO₂-2 group was better than that in the CeO₂-1 and CeO₂-3 groups. These data fully prove that CeO₂ nanoparticles can effectively protect cardiomyocytes and reduce myocardial I/R injury by weakening the oxidative stress response of cardiomyocytes. In addition, it was also found that in terms of myocardial

cell apoptosis index, the three groups injected with different diameters of CeO₂ nanoparticles also had a significant decrease compared with the I/R group, and the difference was statistically significant ($P < 0.05$); and the effect of CeO₂-2 group was better than that of CeO₂-1 and CeO₂-3 group. These further confirm that CeO₂ nanoparticles can reduce the apoptosis caused by myocardial ischemia-reperfusion, and provide a theoretical basis for the treatment and control of myocardial I/R injury.

Conclusions

In this study, a rat model of myocardial I/R injury was prepared and injected with CeO₂ nanoparticles of different diameters to measure and compare the SOD activity, MDA content, and GSH-Px activity; in addition, the myocardial cell apoptosis was measured. The results suggested that CeO₂ nanoparticles can effectively control the degree of myocardial I/R injury, greatly reduce the myocardial cell apoptosis index, and effectively protect rat cardiomyocytes.

However, the mechanism of CeO₂ nanoparticles in myocardial I/R injury had not been fully clarified in clinical applications, and the safety of CeO₂ nanoparticles on the human body had not been effectively verified. Therefore, CeO₂ nanoparticles had not been effectively applied to clinical treatment of myocardial I/R injury. The relevant mechanism and safety had to be further clarified by a large number of in-depth studies. It was hoped that with the development of science and technology, the potential of CeO₂ nanoparticles can be fully tapped so that they can be used in clinics better and safer and benefit the majority of patients.

Acknowledgments

Not applicable.

Conflict interest

The authors declare that they have no conflict of interest.

References

1. Sun X, Gao R, Li W, Zhao Y, Yang H, Chen H, Jiang H, Dong Z, Hu J, Liu J, Zou Y, Sun A, Ge J. Alda-1 treatment promotes the therapeutic effect of mitochondrial transplantation for myocardial ischemia-reperfusion injury. *Bioact Mater* 2021; 6(7): 2058-2069.
2. Chen R, Li W, Qiu Z, Zhou Q, Zhang Y, Li WY, Ding K, Meng QT, Xia ZY. Ischemic Postconditioning-Mediated DJ-1 Activation Mitigate Intestinal Mucosa Injury Induced by Myocardial Ischemia Reperfusion in Rats Through Keap1/Nrf2 Pathway. *Front Mol Biosci* 2021; 8: 655619.
3. Mongkolpathumrat P, Kijawornrat A, Prompant E, Panya A, Chattipakorn N, Barrère-Lemaire S, Kumphune S. Post-Ischemic Treatment of Recombinant Human Secretory Leukocyte Protease Inhibitor (rhSLPI) Reduced Myocardial Ischemia/Reperfusion Injury. *Biomedicines* 2021; 9(4): 422.
4. Huang Y, Sun X, Juan Z, Zhang R, Wang R, Meng S, Zhou J, Li Y, Xu K, Xie K. Dexmedetomidine attenuates myocardial ischemia-reperfusion injury in vitro by inhibiting NLRP3 Inflammasome activation. *BMC Anesthesiol* 2021; 21(1): 104.
5. Li ZX, Li YJ, Wang Q, He ZG, Feng MH, Xiang HB. Characterization of novel lncRNAs in upper thoracic spinal cords of rats with myocardial ischemia-reperfusion injuries. *Exp Ther Med* 2021; 21(4): 352.
6. Wang Q, Li ZX, Li YJ, He ZG, Chen YL, Feng MH, Li SY, Wu DZ, Xiang HB. Identification of lncRNA and mRNA expression profiles in rat spinal cords at various time-points following cardiac ischemia/reperfusion. *Int J Mol Med* 2019; 43(6): 2361-2375.
7. Adili R, Voigt EM, Bormann JL, Foss KN, Hurley LJ, Meyer ES, Veldman AJ, Mast KA, West JL, Whiteheart SW, Holinstat M, Larson MK. In vivo modeling of docosaheptaenoic acid and eicosapentaenoic acid-mediated inhibition of both platelet function and accumulation in arterial thrombi. *Platelets* 2019; 30(2): 271-279.
8. Tejedor S, Dolz-Pérez I, Decker CG, Hernández A, Díez JL, Álvarez R, Castellano D, García NA, Ontoria-Oviedo I, Nebot VJ, González-King H, Igual B, Sepúlveda P, Vicent MJ. Polymer Conjugation of Docosaheptaenoic Acid Potentiates Cardioprotective Therapy in Preclinical Models of Myocardial Ischemia/Reperfusion Injury. *Adv Healthc Mater* 2021; 10(9): e2002121.
9. Han Y, Chen S, Wang H, Peng XM. Electroacupuncture Pretreatment Regulates Apoptosis of Myocardial Ischemia-Reperfusion Injury in Rats Through RhoA/p38MAPK Pathway Mediated by miR-133a-5p. *Evid Based Complement Alternat Med* 2021; 2021: 8827891.

10. Chen X, Wang Y, Xiao ZY, Hou DN, Li DB, Zhang XP. Effect of propofol on myocardial ischemia/reperfusion injury in rats through JAK/STAT signaling pathway. *Eur Rev Med Pharmacol Sci* 2019; 23(14): 6330-6338.
11. Zong C, Wang C, Hu L, Zhang R, Jiang P, Chen J, Wei L, Chen Q. The Enhancement of the Catalytic Oxidation of CO on Ir/CeO₂ Nanojunctions. *Inorg Chem* 2019; 58(20): 14238-14243.
12. Hasanazadeh L, Kazemi Oskuee R, Sadri K, Nourmohammadi E, Mohajeri M, Mardani Z, Hashemzadeh A, Darroudi M. Green synthesis of labeled CeO₂ nanoparticles with ^{99m}Tc and its biodistribution evaluation in mice. *Life Sci* 2018; 212: 233-240.
13. Huang Y, Sun X, Juan Z, Zhang R, Wang R, Meng S, Zhou J, Li Y, Xu K, Xie K. Correction to: Dexmedetomidine attenuates myocardial ischemia-reperfusion injury in vitro by inhibiting NLRP3 Inflammasome activation. *BMC Anesthesiol* 2021; 21(1): 141.
14. Kalakotla S, Jayarambabu N, Mohan GK, Mydin RBSMN, Gupta VR. A novel pharmacological approach of herbal mediated cerium oxide and silver nanoparticles with improved biomedical activity in comparison with Lawsonia inermis. *Colloids Surf B Biointerfaces* 2019; 174: 199-206.
15. Sisubalan N, Ramkumar VS, Pugazhendhi A, Karthikeyan C, Indira K, Gopinath K, Hameed ASH, Basha MHG. ROS-mediated cytotoxic activity of ZnO and CeO₂ nanoparticles synthesized using the *Rubia cordifolia* L. leaf extract on MG-63 human osteosarcoma cell lines. *Environ Sci Pollut Res Int* 2018; 25(11): 10482-10492.
16. Heger J, Hirschhäuser C, Bornbaum J, Sydykov A, Dempfle A, Schneider A, Braun T, Schlüter KD, Schulz R. Cardiomyocytes-specific deletion of monoamine oxidase B reduces irreversible myocardial ischemia/reperfusion injury. *Free Radic Biol Med* 2021; 165: 14-23.
17. Sharifi M, Nazarinia D, Ramezani F, Azizi Y, Naderi N, Aboutaleb N. Necroptosis and RhoA/ROCK pathways: molecular targets of Nesfatin-1 in cardioprotection against myocardial ischemia/reperfusion injury in a rat model. *Mol Biol Rep* 2021; 48(3): 2507-2518.
18. Tian R, Guan X, Qian H, Wang L, Shen Z, Fang L, Liu Z. Restoration of NRF2 attenuates myocardial ischemia reperfusion injury through mediating microRNA-29a-3p/CCNT2 axis. *Biofactors* 2021; 47(3): 414-426.
19. Alavi M, Rai M. Antisense RNA, the modified CRISPR-Cas9, and metal/metal oxide nanoparticles to inactivate pathogenic bacteria. *Cellular, Molecular and Biomedical Reports* 2021;1(2): 52-9.
20. Miri A, Dorani N, Darroudi M, Sarani M. Green synthesis of silver nanoparticles using *Salvadora persica* L. and its antibacterial activity. *Cellular and Molecular Biology* 2016; 62(9): 46-50.
21. Moradi S, Khaledian S, Abdoli M, Shahlaei M, Kahrizi D. Nano-biosensors in cellular and molecular biology. *Cell Mol Biol* 2018;64(5):85-90. doi:10.14715/cmb/2018.64.5.14.
22. Amin ME, Azab MM, Hanora AM, Abdalla S. Antifungal activity of silver nanoparticles on Fluconazole resistant Dermatophytes identified by (GACA) 4 and isolated from primary school children suffering from Tinea Capitis in Ismailia-Egypt. *Cellular and Molecular Biology* 2017; 63(11): 63-7.